Journal of Integrative Neuroscience

J. Integr. Neurosci. **2026**; 25(7): 52117
https://doi.org/10.31083/JIN52117

Original Research

Brain-Wide Connectivity of GLP1R Neurons in the Thalamic Reticular Nucleus

Xiao Zhang[1,2,3,†], Shanghui Zhu[1,2,3,†], Jiangzhong Lan[1,2,3], Shumin Duan[4,5,6], Yong Han[2,3,*], Peng Shi[1,*]

[1]Department of Neurology, The First Affiliated Hospital of Bengbu Medical University, 233004 Bengbu, Anhui, China
[2]Department of Endocrinology, Songjiang Research Institute, Songjiang Hospital Affiliated to Shanghai Jiao Tong University School of Medicine, 201699 Shanghai, China
[3]Shanghai Key Laboratory of Emotions and Affective Disorders (LEAD), Shanghai Jiao Tong University School of Medicine, 201699 Shanghai, China
[4]Liangzhu Laboratory, Zhejiang University, 311121 Hangzhou, Zhejiang, China
[5]MOE Frontier Science Center for Brain Science & Brain-Machine Integration, Zhejiang University, 311121 Hangzhou, Zhejiang, China
[6]State Key Laboratory of Brain-Machine Intelligence, Zhejiang University, 311121 Hangzhou, Zhejiang, China
*Correspondence: hanyong@shsmu.edu.cn (Yong Han); Niandi07@sohu.com (Peng Shi)
[†]These authors contributed equally.

Academic Editor: Jose Donato Junior
Submitted: 21 March 2026 Revised: 22 April 2026 Accepted: 6 May 2026 Published: 23 July 2026

Abstract

Background: Glucagon-like peptide-1 receptor (GLP1R) is a G-protein-coupled receptor recognized for its essential role in metabolic homeostasis and insulin secretion. Emerging evidence suggests that central GLP-1 signaling also modulates sensory information processing and cognitive functions. The thalamic reticular nucleus (TRN) serves as a critical inhibitory hub that filters and prioritizes sensory transmission between the thalamus and the cerebral cortex. We have identified a distinct population of GLP1R-expressing neurons distributed within the TRN; however, their long-range structural connectivity remains largely uncharacterized. **Methods:** In this study we used *Glp1r*-Cre mice combined with viral-genetic tracing strategies to map the whole-brain inputs and outputs of GLP1R-linked neurons. To identify direct monosynaptic inputs, a Cre-dependent retrograde rabies virus system was employed. To delineate the efferent axonal projections, a Cre-dependent synaptophysin-based tracing strategy was employed. **Results:** GLP1R neurons exhibited a distinct rostrocaudal distribution, with most located in the middle region of the TRN. The starter neurons, identified by the colocalization of adeno-associated virus (AAV)-double-floxed inverted orientation (DIO)-enhanced green fluorescent protein (EGFP)-tumor virus A receptor (TVA), AAV-DIO-rabies virus glycoprotein from the CVS-N2c strain (N2cG), and rabies virus (RV)-envelope protein A (EnvA)-glycoprotein-deleted (ΔG)-mCherry, were primarily located in the TRN. Retrograde-labeled neurons were identified across numerous brain regions. Dense clusters of input neurons were observed in the primary and secondary motor cortices (M1 and M2, respectively) and the primary somatosensory cortex (S1). Substantial inputs were observed, including from the ventrolateral (VL), central lateral (CL), and posterior (Po) thalamic nuclei. Additionally, notable presynaptic labeling was detected in subcortical regions such as the zona incerta (ZI) and lateral hypothalamic area (LH), as well as midbrain structures including the substantia nigra pars reticulata (SNR) and the deep mesencephalic nucleus (DpMe). Anterograde synaptophysin-based mapping revealed that TRN^{GLP1R} neurons selectively project to the ventral medial nucleus (VM), paracentral thalamic nucleus (PC), mediodorsal thalamus, lateral part (MDL), and lateral habenula (LHb) nuclei. **Conclusions:** The results confirm the existence of complex long-range afferent and efferent circuits associated with TRN^{GLP1R} neurons, providing a morphological basis for studying their role in integrating metabolic states with sensory gating.

Keywords: thalamic nuclei; glucagon-like peptide-1 receptor; synaptophysin; rabies virus

1. Introduction

The mammalian thalamic reticular nucleus (TRN) is a highly organized γ-aminobutyric acid (GABA)ergic structure located between the cerebral cortex and the dorsal and lateral thalamus, serving as a key interface for thalamocortical communication [1,2,3,4]. Traditionally regarded as local inhibitory pacemakers, TRN neurons regulate thalamic activity through feedforward and feedback inhibition [5,6]. However, emerging evidence has demonstrated that the TRN is not a single inhibitory structure but rather contains molecularly and functionally distinct neuronal populations [7,8]. Recent single-cell transcriptomic and optogenetic studies have revealed that the TRN comprises multiple molecularly defined neuronal subpopulations, including parvalbumin (PV), somatostatin (SST), and vasoactive intestinal peptide neurons [8,9,10,11,12,13,14]. Such cellular diversity underscores the role of the TRN as a key node for the top-down regulation of brain states. Although the TRN has been studied for its role in sensory gating and sleep–wake regulation [7,15,16,17,18,19,20,21], increasing evidence suggests that it may also contribute to metabolic control [22,23].

The glucagon-like peptide-1 receptor (GLP1R) is a key component of the GLP-1 signaling pathway and plays a key role in the regulation of glucose homeostasis and energy metabolism [24,25,26,27]. Beyond its classical metabolic role, GLP1R has also been involved in sensory processing [28,29,30,31]. It has an important role in taste processing, particularly in the modulation of sweet taste sensitivity [30,32], as well as in olfactory-related responses to food detection [29]. GLP1R is also expressed in vagal afferent neurons, where it contributes to gut-brain communication, gastrointestinal stretch, and nutrient sensing [31]. Additionally, activation of GLP1R signaling in nociceptive circuits has been shown to modulate pain hypersensitivity [28], suggesting a role in nociceptive processing. GLP1R signaling also affects cognitive functions such as hippocampal learning, memory, and neuroprotection [33,34,35]. Early evidence showed that GLP1R is expressed in the hippocampus and that activation of central GLP1R signaling enhances spatial learning while protecting neurons from excitotoxic injury [35]. In models of Alzheimer's disease, GLP1R agonists such as exendin-4 and liraglutide have been reported to improve memory performance [33,34]. Interestingly, GLP1R neurons are also detected within the TRN [36], raising the possibility that this subpopulation of TRN neurons may contribute to sensory and sleep-wake regulation. However, the projection patterns and circuit organization of TRN^{GLP1R} neurons have not yet been systematically characterized.

Here, the aim was to obtain a comprehensive view of the long-range connectivity of TRN^{GLP1R} neurons. Previous anatomical studies of TRN circuits were largely performed at the population level and therefore did not resolve the connectivity of genetically defined neuronal subtypes. With the development of viral circuit-tracing tools and imaging methods, it has become possible to map neural circuits across the entire brain in a cell-type-specific manner. Using these techniques, both the inputs and outputs of TRN^{GLP1R} neurons were traced and quantitatively analyzed for their distribution across the brain. The results obtained provide an anatomical basis for future investigations into the functional roles of this neuronal population.

2. Materials and Methods

2.1 Animals

Total 5 adult male *Glp1r*-Cre mice (2–4 months old) were obtained by mating heterozygous *Glp1r*-Cre mice with C57BL/6 wild-type mice. The heterozygous *Glp1r*-Cre mice (JAX Stock #029283, The Jackson Laboratory, Bar Harbor, ME, USA) and Ai9 mice (JAX Stock #007909) were originally purchased from the Jackson Laboratory. Mice were maintained under controlled temperature at 22–24 ℃ and humidity at approximately 50% on a 12-h light/dark cycle with food and water available *ad libitum*.

2.2 Monosynaptic Retrograde Tracing

To identify direct inputs to TRN^{GLP1R} neurons, a Cre-dependent rabies virus tracing strategy was used. Helper adeno-associated virus (AAV) vectors carryingdouble-floxed inverted orientation (DIO)-enhanced green fluorescent protein (EGFP)-tumor virus A receptor (TVA) (BC-0041, Brain Case, Wuhan, Hubei, China) and DIO-rabies virus glycoprotein from the CVS-N2c strain (N2cG) (BC-0442, Brain Case) were stereotaxically injected into the TRN. After two weeks, envelope protein A (EnvA)-pseudotyped, glycoprotein-deleted rabies virus (BC-RV-CVS-EnvA471, Brain Case) expressing mCherry was delivered to the same location. Starter neurons were identified by co-expression of EGFP and mCherry. Monosynaptically connected presynaptic neurons were labeled with mCherry.

2.3 Anterograde Axon Tracing

To define output projections of TRN^{GLP1R} neurons, a Cre-dependent AAV vector expressing DIO-mRuby-thosea asigna virus 2A peptide (T2A)-Synaptophysin-EGFP (BC-1025, Brain Case) was injected into the TRN of *Glp1r*-Cre mice. After three weeks of expression, whole-brain coronal sections were analyzed to determine axonal distribution patterns.

2.4 Brain Stereotaxic Injection

Glp1r-Cre mice were anesthetized with isoflurane (3–5% for induction and 1.5% for maintenance, with a flow rate of 2 L/min; R510, RWD, Shenzhen, Guangdong, China) and fixed in a stereotaxic apparatus (HOYI-M, RWD). After exposing the skull, a small craniotomy was made above the TRN. A glass micropipette (GC-3.5, RWD) was positioned at the TRN using stereotaxic coordinates relative to bregma (anteroposterior (AP), –0.7 mm; mediolateral (ML), –1.1 mm; dorsoventral (DV), –3.8 mm; coordinates adjusted according to the mouse brain atlas).

To enable monosynaptic retrograde tracing, two Cre-dependent helper AAVs (AAV-EF1α-DIO-EGFP-TVA and AAV-EF1α-DIO-N2cG, mixed at a 1:1 ratio) were first injected into the TRN. A total volume of 100 nL viral solution was delivered at a rate of 0.01 μL/min using a microsyringe pump controller (R-480, RWD). After completion of the injection, the micropipette was left in place for 10–15 min to allow viral diffusion before being slowly withdrawn.

After viral infection for two weeks, 100 nL of RV-EnvA-ΔG-mCherry was injected into the same location. Mice were maintained for an additional seven days to allow rabies virus propagation and labeling of presynaptic neurons before being sacrificed for brain tissue collection and histological analysis.

2.5 Histology

Mice were placed individually in a euthanasia chamber, and 100% CO_2 from a compressed gas cylinder was introduced at a flow rate of 50% displacement of the cham-

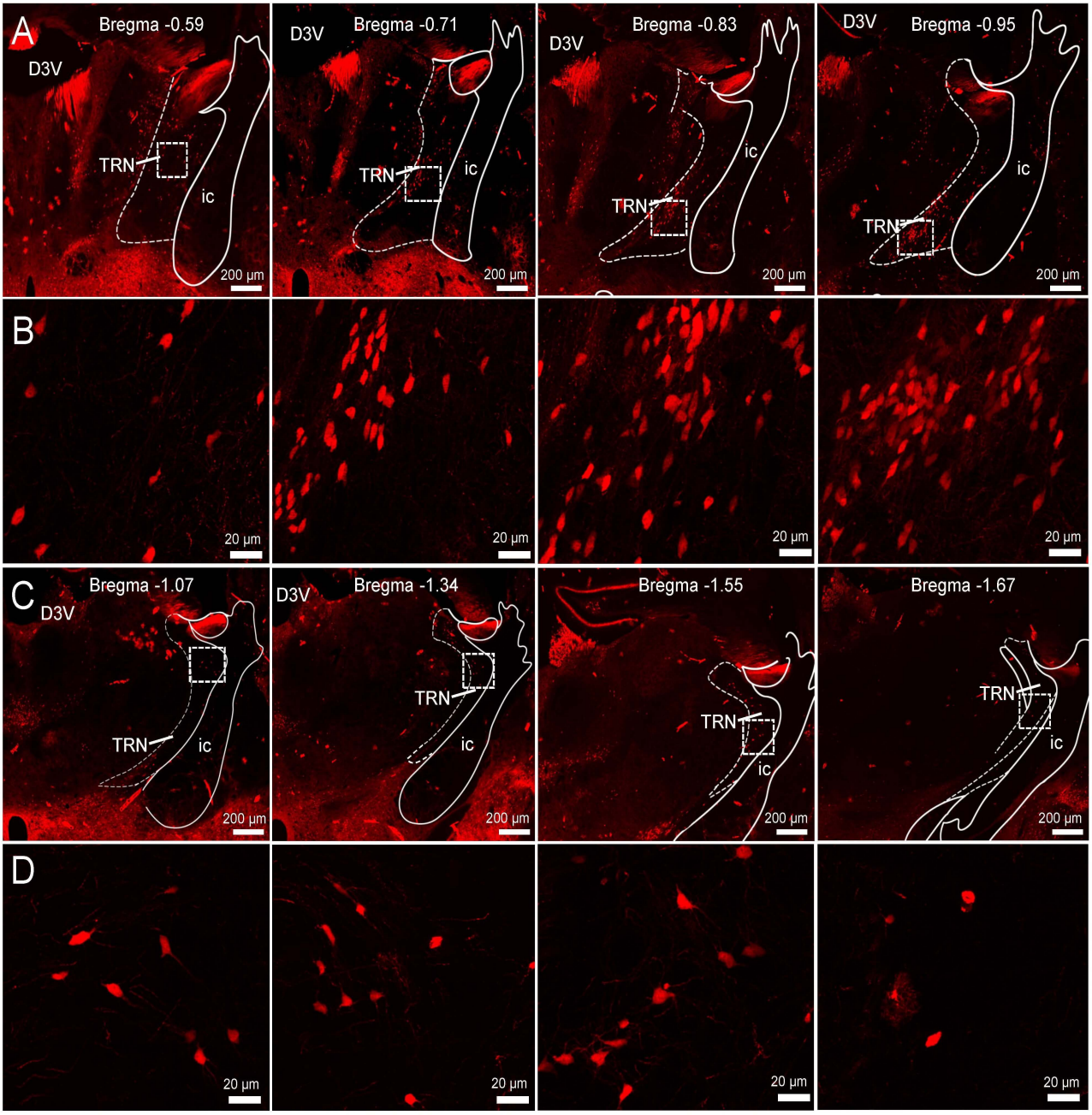

Fig. 1. Spatial distribution of GLP1R neurons within the TRN. Representative coronal brain sections from a *Glp1r*-Cre;Ai9 reporter mouse illustrating the distribution of tdTomato-labeled TRN^{GLP1R} neurons throughout the rostrocaudal axis of the TRN. Sections are arranged from anterior to posterior relative to the bregma. (A,C) Low-magnification images showing the overall distribution of GLP1R-expressing neurons within the TRN at different sections. The white dashed boxes indicate the regions shown at higher magnification in (B,D). (B,D) High-magnification views of the boxed areas in (A) and (C) show the morphology of TRN^{GLP1R} neurons. Scale bar in (A,C), 200 μm; scale bar in (B,D), 20 μm. Irregular dashed outlines indicate the boundary of the TRN, and irregular solid outlines indicate the adjacent internal capsule (ic). GLP1R, glucagon-like peptide-1 receptor; TRN, thalamic reticular nucleus; D3V, dorsal third ventricle.

ber volume per minute with CO_2. The CO_2 was added to the existing air in the chamber until respiration ceased. Mice remained in the chamber for an additional 5 min, and euthanasia was confirmed by the absence of respiration and reflexes before transcardial perfusion. The mice were then transcardially perfused with 0.1 mol/L phosphate-buffered saline (PBS, pH 7.4; B548117, Sangon Biotech, Shanghai, China) followed by freshly prepared 4% paraformaldehyde (AG2161, ACMEC, Shanghai, China) dissolved in PBS. After perfusion, brains were carefully removed and

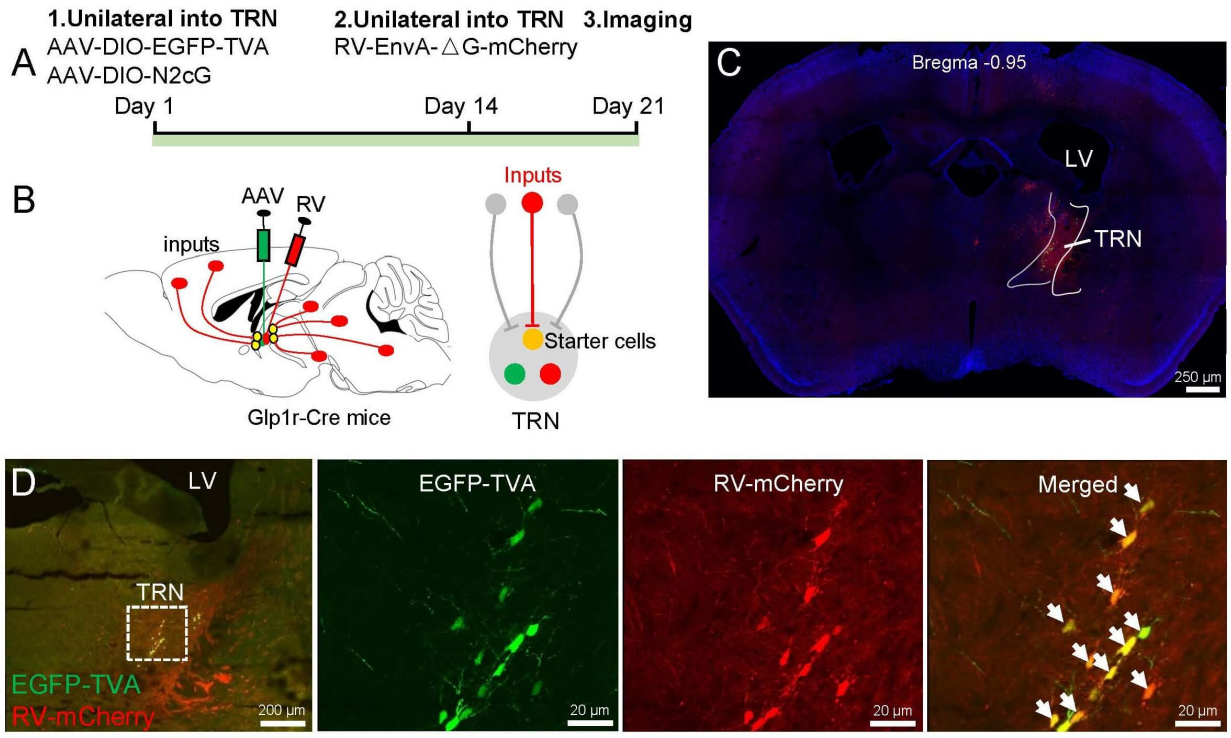

Fig. 2. Experimental procedures for retrograde monosynaptic tracing to identify direct inputs to TRN^{GLP1R} neurons. (A) Schematic illustration of the experimental strategy. Monosynaptic retrograde rabies virus tracing was used to map the presynaptic inputs to GLP1R neurons in the TRN. (B) Diagram of the stereotaxic injection procedure showing delivery of AAV helper viruses (AAV-DIO-EGFP-TVA and AAV-DIO-N2cG) followed by RV-EnvA-ΔG-mCherry into the TRN of *Glp1r*-Cre mice. (C) Representative image from the unilateral rabies tracing experiment showing starter cells (yellow). Nuclei were stained with DAPI. Scale bar, 250 μm. (D) High-magnification images of the TRN showed that viral expression was confined to the injection region. Starter neurons co-expressing EGFP and mCherry are indicated by arrows in the enlarged view. Scale bar, 200 μm; scale bar in enlarged view of the TRN (right), 20 μm. AAV, adeno-associated virus; LV, lateral ventricle; DIO, double-floxed inverted orientation; EGFP, enhanced green fluorescent protein; TVA, tumor virus A receptor; N2cG, rabies virus glycoprotein from the CVS-N2c strain; RV, rabies virus; EnvA, envelope protein A; DAPI, 4′,6-diamidino-2-phenylindole.

post-fixed in the same fixative at 4 °C for approximately six hours. Subsequently, the tissues were transferred to a 30% sucrose solution in PBS and maintained at 4 °C for about 48 h until the brains sank. Following cryoprotection, brains were embedded in optimal cutting temperature (OCT, Sakura Finetek USA, Inc., Torrance, CA, USA) compound and sectioned coronally at a thickness of 30 μm using a freezing cryostat (Leica Biosystems, Nussloch, Baden-Württemberg, Germany). Whole-brain mRNA expression data for *Glp1r* were referenced from the Allen Brain Atlas [37] *in situ* hybridization database, experiment ID 74511737.

2.6 Image Acquisition and Data Analysis

Whole-brain coronal sections were imaged using an inverted confocal microscope (FV3000, Olympus, Tokyo, Japan). To ensure clear separation of fluorescent signals, appropriate excitation lasers and emission filters were selected during imaging. EGFP was excited at 488 nm with emissions collected between 500–530 nm, whereas mCherry was excited at 594 nm with emissions detected within the 600–650 nm range. Image acquisition was performed using the FLUOVIEW imaging software (FV31S-SW, Olympus). Image acquisition parameters, including brightness and contrast, were adjusted during imaging to optimize signal detection. The boundaries of individual brain nuclei were identified according to the mouse brain atlas and manually outlined for subsequent analysis. mCherry-positive neurons were manually counted from the projected images of each section. Only animals with accurately targeted injection sites were included in the analysis, and data from these mice were used for all quantitative measurements and figures. These experiments represent biological replication. The representative fluorescence images presented in this study were acquired from endogenous fluorescent signals, including tdTomato expressed in transgenic mice and EGFP or mCherry expressed by viral vectors.

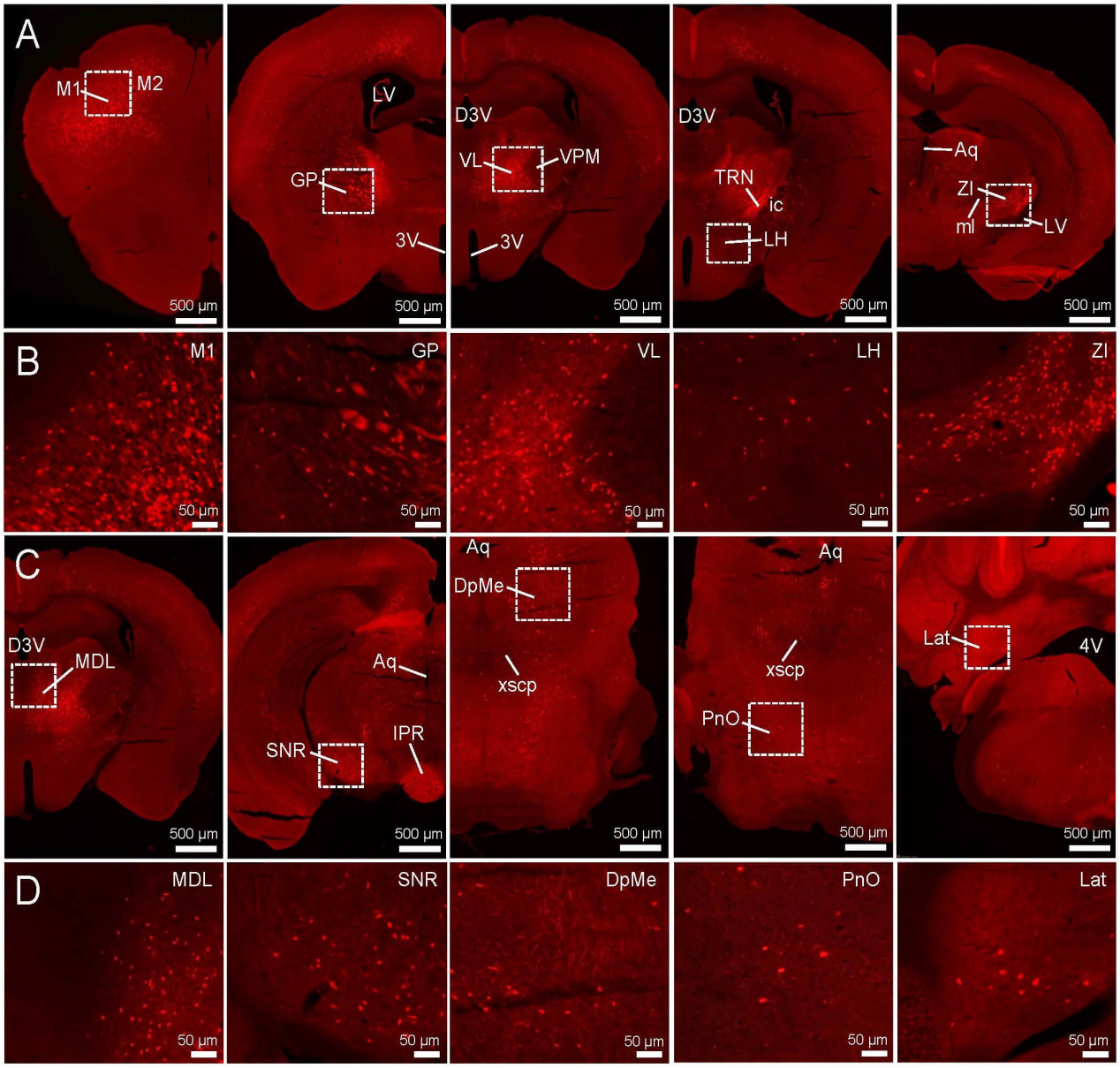

Fig. 3. Brain regions receiving monosynaptic inputs to TRN^{GLP1R} neurons. Representative images showing rabies virus–labeled presynaptic neurons in selected brain regions. Images are arranged from cortical to subcortical and brainstem regions to illustrate the inputs across the brain. (A,C) Low-magnification images showing the mCherry-positive neurons providing direct monosynaptic inputs to GLP1R neurons in the TRN. The white dashed boxes indicate the regions shown at higher magnification in (B,D). (B,D) High-magnification views of the boxed areas in (A) and (C). Scale bar in (A,C), 500 μm; scale bar in (B,D), 50 μm. M1, primary motor cortex; GP, globus pallidus; VL, ventrolateral thalamic nucleus; LH, lateral hypothalamus; ZI, zona incerta; MDL, mediodorsal thalamic nucleus, lateral part; SNR, substantia nigra pars reticulata; DpMe, deep mesencephalic nucleus; PnO, pontine reticular nucleus, oral part; Lat, lateral (dentate) cerebellar nucleus; M2, secondary motor cortex; VPM, ventral posteromedial nucleus of the thalamus; IPR, interpeduncular nucleus, rostral part.

3. Results

3.1 Distribution of GLP1R Neurons in the TRN

To determine whether GLP1R-expressing neurons are present in the TRN, tdTomato fluorescence was examined in *Glp1r*-Cre;Ai9 mice, in which GLP1R-expressing neurons are genetically labeled. The tdTomato-positive neurons were observed in multiple brain regions, including TRN, showing a distinct population of GLP1R-expressing neurons (Fig. 1). In addition, RNAscope *in situ* hybridization further confirmed the presence of *Glp1r* mRNA in the TRN (**Supplementary Fig. 1**), providing direct evidence that GLP1R is expressed in this region.

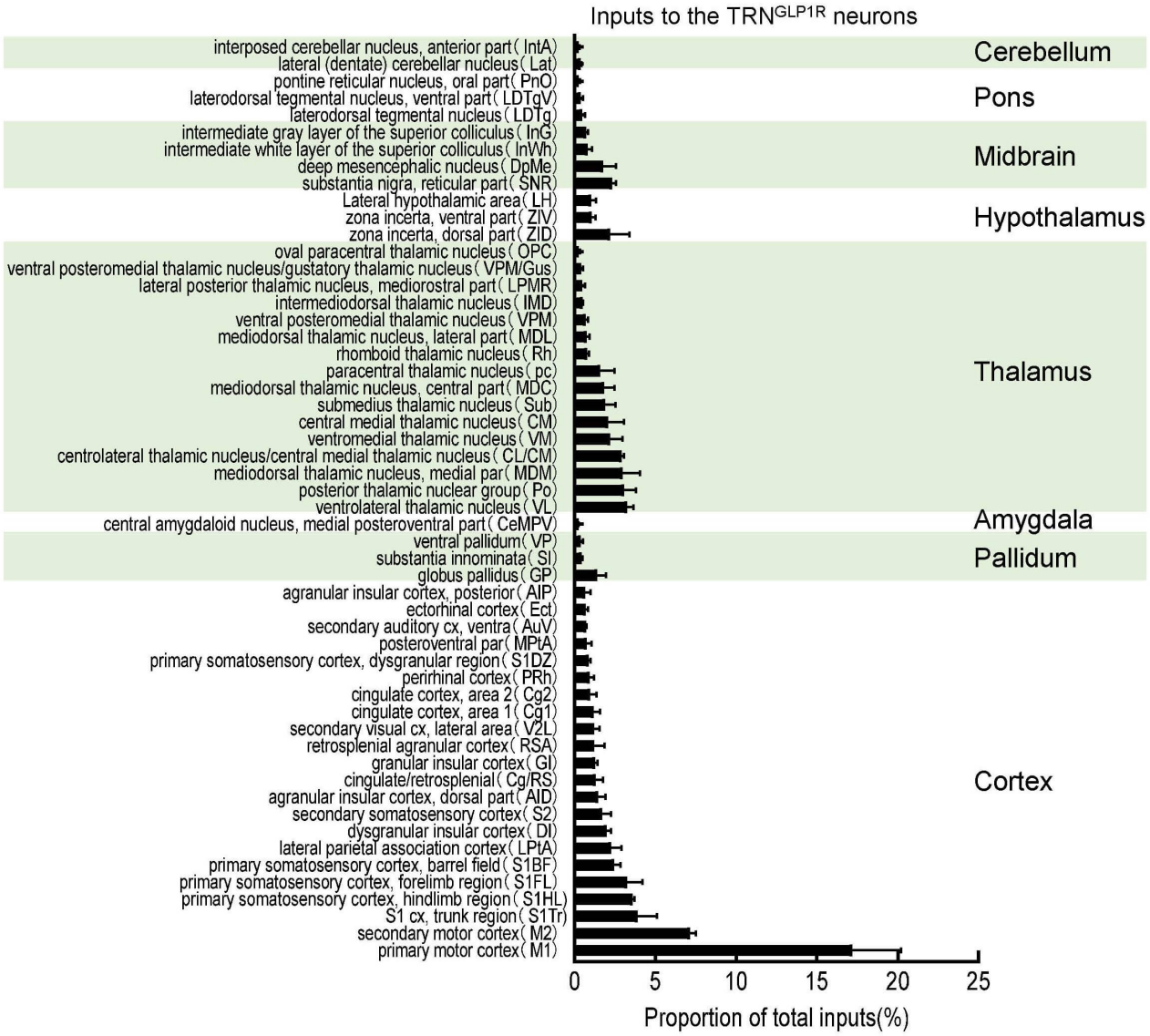

Fig. 4. Quantitative analysis of the whole-brain monosynaptic inputs to TRN^{GLP1R} neurons. Data are presented as the percentage of retrogradely labeled neurons across 54 identified brain regions from 3 mice. These regions are categorized into eight major anatomical structures: cortex, pallidum, amygdala, thalamus, hypothalamus, midbrain, pons, and cerebellum. Error bars represent mean ± s.e.m.

Representative coronal sections from bregma –0.59 to –1.67 mm revealed that GLP1R-expressing neurons were distributed along the rostrocaudal axis of the TRN. However, the TRN^{GLP1R} neurons had a different distribution pattern from rostral to caudal TRN. In the rostral TRN (bregma –0.59 mm), GLP1R-expressing neurons were sparse within the nucleus (Fig. 1A,B). As the sections moved caudally (bregma –0.71 to –0.83 mm), the number of GLP1R-expressing neurons increased, and more densely distributed within the TRN (Fig. 1A,B). Interestingly, the GLP1R-expressing neurons were located closely against the thalamus, forming a dense distribution in the ventral part of the TRN. In the middle TRN (bregma –0.95 mm), GLP1R-expressing neurons were particularly abundant within the ventral part of the nucleus (Fig. 1A,B). In the caudal TRN, GLP1R-expressing neurons became more sparsely distributed, while still maintaining the typical longitudinal pattern of the nucleus (Fig. 1C,D). These results demonstrate that GLP1R-expressing neurons are well organized in the TRN and show a defined rostrocaudal distribution pattern, providing an anatomical basis for neural mapping experiments.

To determine the subtypes of TRN^{GLP1R} neurons, immunostaining for parvalbumin (PV) and somatostatin (SST) in *Glp1r*-Cre;Ai9 mice was performed (**Supplementary Fig. 2**). Only a small population of GLP1R neurons colocalized with PV, whereas a much larger proportion colocalized with SST. These results indicate that GLP1R is preferentially expressed in the SST neurons rather than PV.

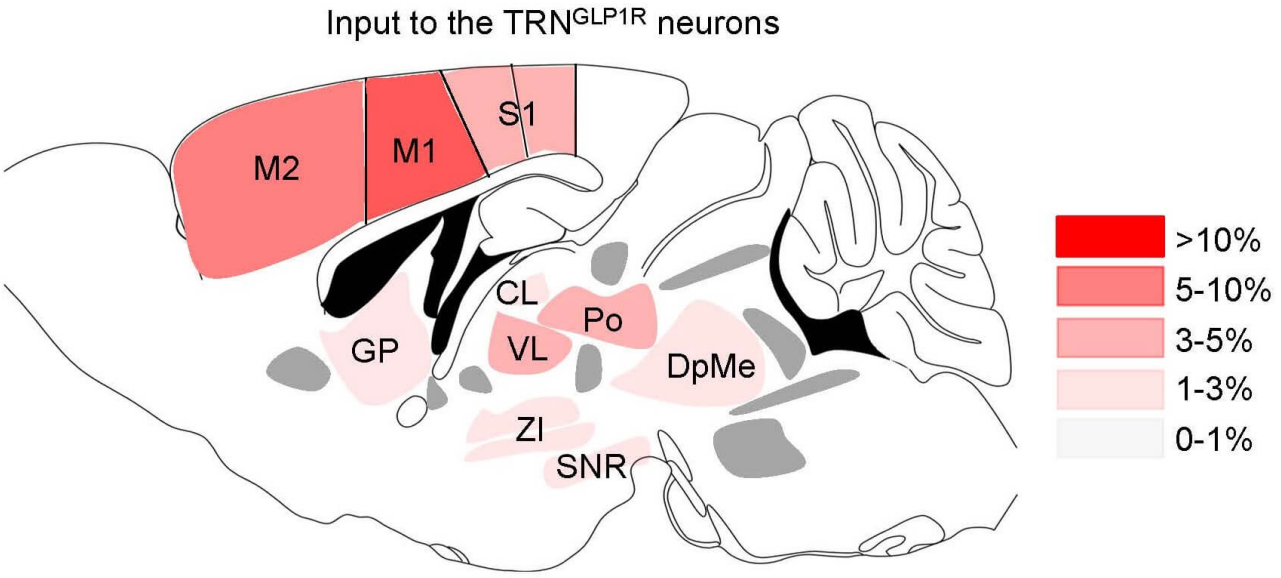

Fig. 5. Schematic summary of major presynaptic inputs to TRN^{GLP1R} neurons. Brain regions providing monosynaptic inputs to TRN^{GLP1R} neurons are illustrated on a sagittal brain diagram. The color gradient indicates the relative proportion of presynaptic neurons contributed by each region, expressed as a percentage of the total labeled inputs. Darker colors represent regions with stronger inputs. CL, central lateral thalamic nucleus; Po, posterior thalamic nuclear group; S1, primary somatosensory cortex.

3.2 Verification of Viral Injection Sites in the TRN

To investigate the long-range connectivity of TRN^{GLP1R} neurons, Cre-dependent viral tracing strategies were employed in *Glp1r*-Cre mice. The helper viruses AAV- EF1α-DIO-EGFP-TVA and AAV-EF1α-DIO-N2cG were stereotaxically injected into the TRN, followed by the injection of RV-EnvA-ΔG-mCherry into the same site after a period of two weeks (Fig. 2A).

In this experiment, only animals with injection sites restricted to the TRN were included in the further analysis. The injection sites were verified by examining EGFP and mCherry fluorescence in coronal brain sections (Fig. 2B). Starter neurons were defined by the colocalization of EGFP and mCherry. Of note, these starter cells were restricted to the TRN and found in the middle part of TRN, approximately from bregma –0.83 to –1.07 mm (Fig. 2C,D and **Supplementary Fig. 3**). These results confirm the anatomical specificity of the viral tracing strategy, providng a reliable basis for circuit tracing.

3.3 Whole-Brain Distribution of Presynaptic Neurons Projecting to TRN^{GLP1R} Neurons

Rabies virus-mediated retrograde tracing revealed that neurons projecting to TRN^{GLP1R} neurons were widely distributed across multiple brain regions. Presynaptic neurons were detected in the cerebral cortex, thalamus, hypothalamus, midbrain, pons, and cerebellum, indicating that TRN^{GLP1R} neurons receive convergent inputs from diverse brain regions (Fig. 3).

Within the cerebral cortex, retrogradely labeled neurons were primarily located in the motor cortex (M1 and M2), somatosensory cortex (S1), and medial prefrontal cortex, including the cingulate and retrosplenial areas (Fig. 3A,B). These cortical neurons were predominantly distributed in layers V and VI, a pattern consistent with previous studies of cortical projections to the TRN [38,39].

In the subcortical regions, the thalamus emerged as the most prominent source of input. Labeled neurons were widely distributed across various thalamic nuclei, such as the ventrolateral (VL), posterior (Po), and mediodorsal (MD) nuclei (Fig. 3A,B). Moderate labeling was also observed in the hypothalamus, specifically within the zona incerta (ZI) and lateral hypothalamus (LH), as well as in the basal ganglia, including the globus pallidus (GP) and ventral pallidum (Fig. 3A,B).

For the midbrain and brainstem, the inputs were also observed in the substantia nigra pars reticulata (SNR), deep mesencephalic nucleus (DpMe) and pontine reticular nucleus (PnO) (Fig. 3C,D). Additionally, presynaptic neurons were identified in the cerebellar nuclei (Fig. 3C,D), while the TRN^{GLP1R} neurons received bilateral inputs, most of these presynaptic neurons were located in the ipsilateral region relative to the injection site.

The whole-brain distribution of presynaptic inputs to TRN^{GLP1R} neurons was quantified by counting mCherry-labeled neurons in each brain region (Figs. 4,5). To compare input strength across nuclei, the number of labeled neurons in each brain region was normalized to the total num-

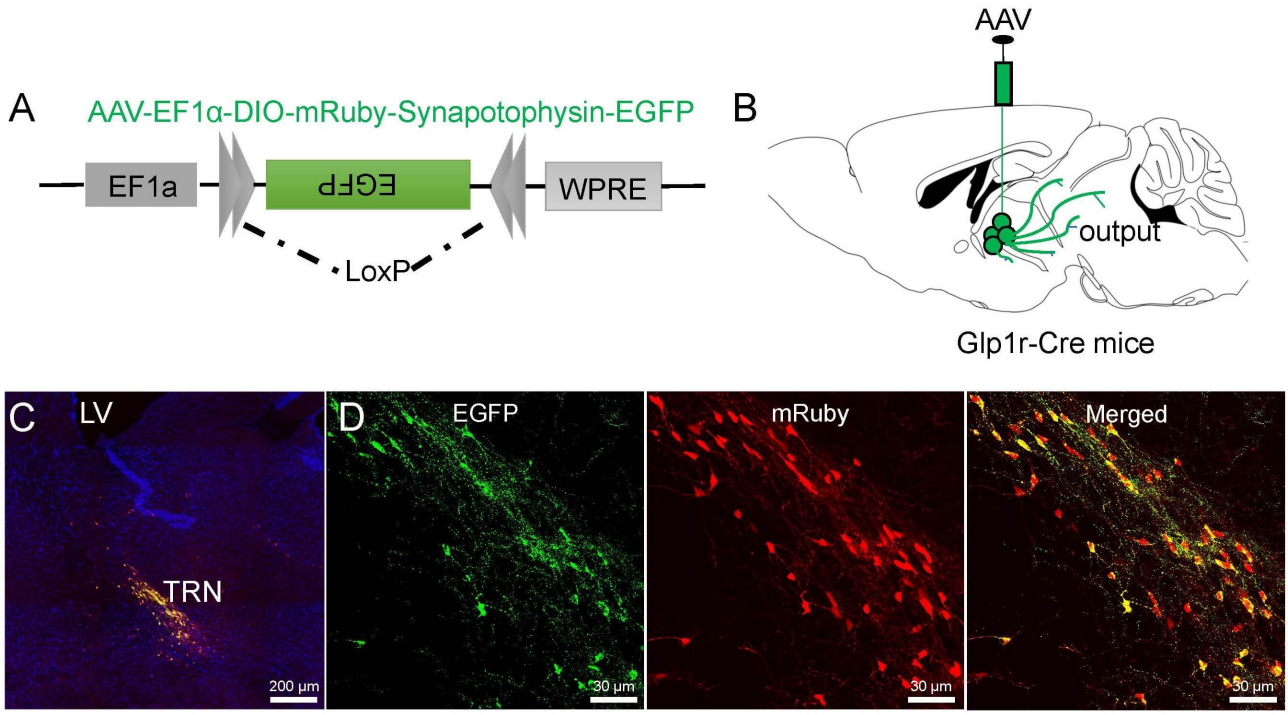

Fig. 6. Strategy for mapping the efferent projections of TRN^{GLP1R} neurons. (A) Schematic diagram of the Cre-dependent AAV-EF1α-DIO-mRuby-Synaptophysin-EGFP used to label TRN^{GLP1R} neurons and their presynaptic terminals. mRuby labels infected neuronal somata and axons, whereas synaptophysin-EGFP is expressed in presynaptic boutons, allowing to map downstream targets. (B) Experimental scheme showing injection of the AAV into the TRN of *Glp1r*-Cre mice to trace the downstream projections of TRN^{GLP1R} neurons. (C) Representative image showing expression of mRuby (red) and synaptophysin-EGFP (green) in the TRN. Scale bar, 200 μm. (D) High-magnification images of TRN^{GLP1R} neurons from C. Scale bar, 30 μm. LV, lateral ventricle; EF1α, elongation factor 1 alpha; WPRE, woodchuck hepatitis virus post-transcriptional regulatory element; LoxP, locus of X-over P1.

ber of mCherry-labeled neurons in the corresponding brain. Using this criterion, 54 nuclei were identified that each contributed, on average, more than 0.2% of the total monosynaptic inputs (Fig. 4). Among these regions, the greatest number of inputs to TRN^{GLP1R} neurons came from the M1, which accounted for 17.19% ± 3.02% of the total inputs. Substantial inputs were also observed from the M2 (7.14% ± 0.39%) and the VL (3.25% ± 0.40%). Overall, this brain-wide quantification of presynaptic neurons revealed the input architecture for TRN^{GLP1R} neurons and indicated several candidate regions for further functional study (Figs. 4,5).

3.4 Axonal Projections From TRN^{GLP1R} Neurons

To examine the efferent projections of TRN^{GLP1R} neurons, AAV-DIO-mRuby-T2A-Synaptophysin-EGFP was injected into the TRN of *Glp1r*-Cre mice to label the axonal terminals of these neurons (Fig. 6A,B). The cell bodies of TRN^{GLP1R} neurons were labeled by mRuby and EGFP (Fig. 6C,D). Meanwhile, the synaptophysin-EGFP targets presynaptic terminals and maps downstream targets of TRN^{GLP1R} neurons. The results showed EGFP-positive axonal fibers were observed in a few downstream targets (Fig. 7 and **Supplementary Fig. 4**), including the ventral medial nucleus (VM), paracentral thalamic nucleus (PC) and mediodorsal thalamic nucleus (MDL), suggesting that TRN^{GLP1R} neurons exert inhibitory effects on thalamic relay neurons.

In addition to thalamic targets, moderate projections were also observed in LHb (Fig. 7B), a key hub for processing aversive emotions and reward behaviors. These projections are consistent with the known GABAergic output of TRN neurons. This result indicates that TRN^{GLP1R} neurons may potentially integrate sensory-motor information from the thalamus with the limbic system's processing of negative valence and metabolic states.

4. Discussion

The existence of GLP1R-expressing neurons in the TRN is supported by several lines of evidence. Previous studies by Cork and colleagues [36], as well as observations from Graham and colleagues [40], have suggested GLP1R expression in or near the TRN. In the present study, we confirmed the GLP1R-expressing neurons in the TRN by RNAscope analysis, which is consistent with the *in situ* hybridization data from the Allen Brain Atlas [37]. We further examined the distribution pattern of GLP1R neurons in the

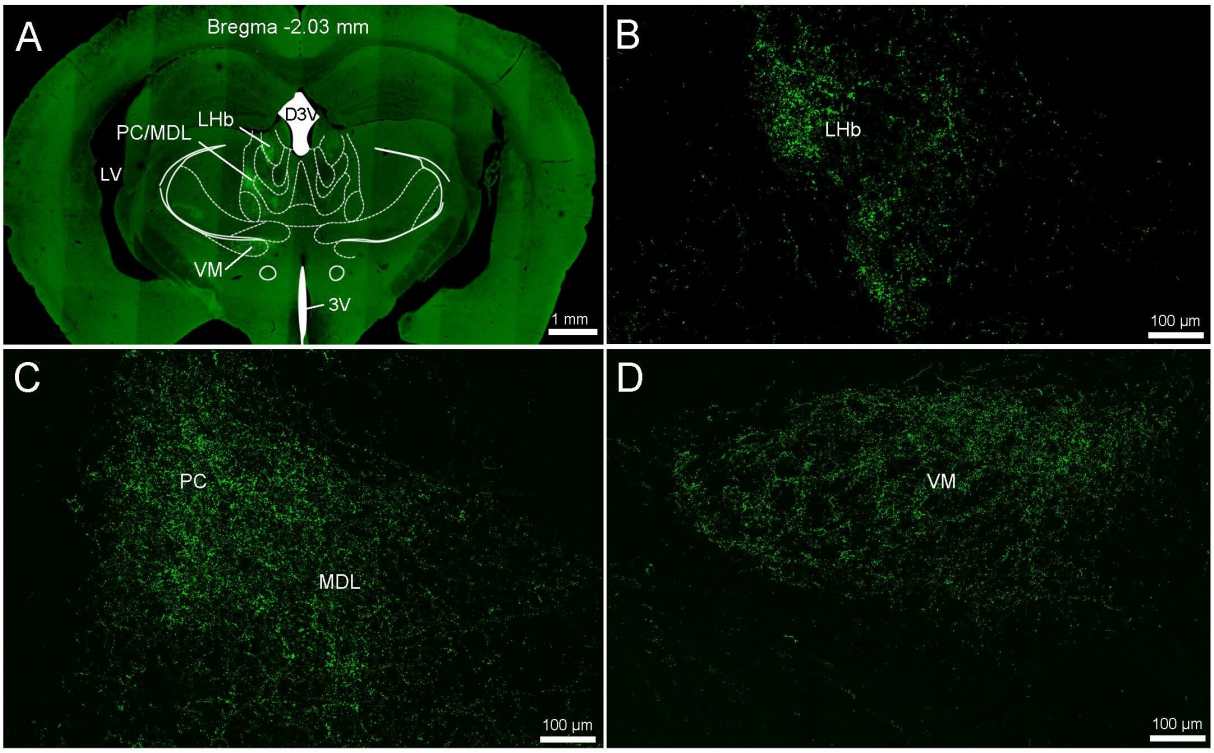

Fig. 7. The axonal projections from TRN^{GLP1R} neurons in downstream target. (A) Representative coronal brain sections show the distribution of axonal projections from TRN^{GLP1R} neurons. Axonal terminals were labeled by synaptophysin-EGFP following injection of the Cre-dependent AAV reporter into the TRN of *Glp1r*-Cre mice. Images illustrate the projection of TRN^{GLP1R} neurons. Scale bar, 1 mm. (B–D) Higher-magnification images showing dense projection in LHb, PC/MDL and VM. Scale bar in (B–D), 100 μm. VM, ventromedial thalamic nucleus; LHb, lateral habenular nucleus; PC, paracentral thalamic nucleus.

TRN. Together, these findings confirm that GLP1R is expressed in the TRN and preferentially colocalizes with SST.

In the current study, the long-range afferent and efferent connectivity of TRN^{GLP1R} neurons was systematically characterized using cell-type-specific viral tracing strategies. By combining retrograde monosynaptic rabies tracing with Cre-dependent anterograde labeling, a whole-brain connectivity map of TRN^{GLP1R} neurons was generated. It should be noted that the starter cells labeled by rabies were mainly restricted to the middle portion of the TRN rather than the whole TRN. Therefore, the tracing results represent the connectivity of a restricted group of TRN^{GLP1R} neurons. Future studies will be needed to determine whether more rostral or caudal TRN^{GLP1R} neurons show distinct connectivity patterns.

Results reveal that TRN^{GLP1R} neurons receive extensive inputs from cortical, thalamic, and midbrain regions and send projections primarily to thalamic relay nuclei and LHb. These findings provide an anatomical framework for understanding how GLP1R neurons in the TRN may integrate metabolic and arousal-related signals with thalamocortical activity.

One of the largest sources of input to TRN^{GLP1R} neurons came from the cerebral cortex, with especially dense labeling in the motor cortex (including M1 and M2) and S1 [38,41]. These retrogradely labeled cortical neurons were mainly located in the deep layers of the cortex, corresponding to layer V and part of layer VI, which are known to provide corticothalamic projections [38,42,43,44]. Previous studies have shown that corticothalamic projections from these layers are essential for modulating thalamic excitability and shaping both sensory and motor processing [45,46,47,48,49]. The dense distribution of labeled neurons across M1, M2, and S1 suggests that TRN^{GLP1R} neurons are potentially positioned to integrate top-down motor information with bottom-up sensory feedback. Therefore, cortical projections to TRN^{GLP1R} neurons may participate in the higher-order cortical control of thalamic inhibitory gating, potentially regulating attention, sensation, sleep, and motor-related thalamic oscillations [50,51,52,53,54].

In addition to cortical inputs, the thalamus is another important brain region that projects to TRN^{GLP1R} neurons. TRN^{GLP1R} neurons received many projections from several thalamic regions, including the VL, Po, and MD. This robust thalamic input suggests the thalamus-TRN pathway is key to the fine regulation of thalamic output and oscillatory activity.

The hypothalamus also showed a moderate afferent distribution from TRN^{GLP1R} neurons, particularly within the ZI and LH, which are well-known regulators of feeding behavior, arousal, and energy homeostasis [55,56,57,58,59,60]. Nevertheless, considering the established functions of the TRN in cognition and arousal, TRN^{GLP1R} neurons may contain a previously unrecognized cell population through which GLP-1 signaling influences thalamocortical dynamics and behavioral state. Future studies will be required to determine whether these neurons are involved in sensory regulation, attention processing, arousal, and cognition.

This study also revealed inputs from midbrain and brainstem nuclei, notably the SNR and DpMe. The projection from the SNR, a major output station of the basal ganglia [61], suggests that TRN^{GLP1R} neurons may serve as a key node in the basal ganglia-thalamic pathway, potentially gating motor-related information. The DpMe is known to participate in REM sleep regulation [62], here the DpMe projection to TRN^{GLP1R} neurons may also regulate the sensory role of the thalamus, with the pathway from DpMe projection toTRN^{GLP1R} also potentially participating in the dynamic suppression of sensory processing during sleep.

In contrast to the widespread inputs of TRN^{GLP1R} neurons, these neurons exhibit limited downstream targets, including the VM, PC/MDL, and LHb. Given that the VM is a critical hub for basal ganglia-thalamocortical loops and the MDL is involved in cognitive processes [63,64,65], the obvious projection to the VM and MDL nucleus from TRN^{GLP1R} neurons underscores the role of these neurons in the control of motor-related behaviors and executive functions. The LHb is a well-established center for processing negative valence, aversion, and stress [66,67]. By targeting the LHb, TRN^{GLP1R} neurons may provide a pathway through which metabolic signals directly influence motivational states and emotional behaviors [11]. While they cannot be excluded, the possibility of sparse projections to other brain regions, the VM, MDL, and LHb, is still recognized as the primary downstream targets of TRN^{GLP1R} neurons.

A potential limitation of the present study is the specificity of Cre labeling in the *Glp1r*-Cre line, as recent work has suggested that Cre activity in some GLP1R reporter systems may partially reflect transient developmental expression rather than adult Glp1r expression [68]. In this study, however, RNAscope analysis confirmed the presence of *Glp1r* mRNA in the TRN. This observation is further supported by *in situ* hybridization data from the Allen Mouse Brain Atlas, which also indicates Glp1r expression in this region of the adult mouse brain. These data strengthen the interpretation that the labeled population here represents a neuronal subpopulation with endogenous Glp1r expression in the TRN. Colocalization of TRN^{GLP1R} neurons with GABAergic subtype markers, such as PV and SST, suggests that these neurons exhibit cellular heterogeneity. Nevertheless, future studies are still needed to more precisely define the heterogeneity of TRN^{GLP1R} neurons. Another limitation is that these data do not directly establish the functional roles of the TRN^{GLP1R} neurons in sleep-wake regulation, sensory gating, or cognition, although we provide a brain-wide map of the inputs and outputs of TRN^{GLP1R} neurons. Therefore, further functional studies will be needed to determine the roles of TRN^{GLP1R} circuits.

Taken together, these data indicate that TRN^{GLP1R} neurons represent a key intersection of brain network signals from the cortex, thalamus, hypothalamus, and brainstem. This connectivity architecture suggests that TRN^{GLP1R} neurons may play a role in coordinating sensory signals with thalamocortical activity and behavioral state.

5. Conclusions

The present study provides anatomical evidence for the brain-wide connectivity of TRN^{GLP1R} neurons. It showed that TRN^{GLP1R} neurons receive widespread inputs from cortical and thalamic regions and project to limited downstream nuclei, suggesting that they may participate in the integration of sensory and arousal-related information within thalamic networks. These findings identify several previously unrecognized neural circuits of TRN^{GLP1R} neurons and provide another neuronal type for understanding how sensory signals may influence thalamocortical function. The functional roles of these pathways remain to be determined.

Availability of Data and Materials

All data reported in this paper will also be shared by the lead contact upon request.

Author Contributions

YH, SD and PS designed the study; XZ, SZ and JL conducted the experiments and the data analysis; YH wrote the manuscript; SD, XZ and SZ edited the manuscript; SD, YH and PS supervised all aspects of the project. All authors contributed to editorial changes in the manuscript. All authors read and approved the final manuscript. All authors have participated sufficiently in the work and agreed to be accountable for all aspects of the work.

Ethics Approval and Consent to Participate

All animal experiments were conducted in accordance with the Institutional Animal Care and Use Committee of Shanghai Jiao Tong University School of Medicine and the ARRIVE guidelines 2.0. The research protocol was approved by the Ethics Committee of Shanghai Jiao Tong University School of Medicine (Ethics Approval Number: ACE-003-2023).

Acknowledgment

We gratefully acknowledge the assistance from Songjiang Research Institute Animal Facility and Optical Imaging Core.

Funding

This work was supported by grants from Natural Science Foundation of Shanghai (Grant No. 24ZR1463100 to Yong Han).

Conflicts of Interest

The authors declare no conflicts of interest.

Declaration of AI and AI-Assisted Technologies in the Writing Process

During the preparation of this work the authors used ChatGPT-5.4 to check spelling and grammar. After using this tool, the authors reviewed and edited the content as needed and take full responsibility for the content of the publication.

Supplementary Material

Supplementary material associated with this article can be found, in the online version, at https://doi.org/10.31083/JIN52117.

References

[1] Huguenard JR, Prince DA. A novel T-type current underlies prolonged Ca(2+)-dependent burst firing in GABAergic neurons of rat thalamic reticular nucleus. The Journal of Neuroscience: the Official Journal of the Society for Neuroscience. 1992; 12: 3804–3817. https://doi.org/10.1523/JNEUROSCI.12-10-03804.1992

[2] Kim U, Sanchez-Vives MV, McCormick DA. Functional dynamics of GABAergic inhibition in the thalamus. Science. 1997; 278: 130–134. https://doi.org/10.1126/science.278.5335.130

[3] de Biasi S, Frassoni C, Spreafico R. GABA immunoreactivity in the thalamic reticular nucleus of the rat. A light and electron microscopical study. Brain Research. 1986; 399: 143–147. https://doi.org/10.1016/0006-8993(86)90608-6

[4] Yen CT, Conley M, Hendry SH, Jones EG. The morphology of physiologically identified GABAergic neurons in the somatic sensory part of the thalamic reticular nucleus in the cat. The Journal of Neuroscience: the Official Journal of the Society for Neuroscience. 1985; 5: 2254–2268. https://doi.org/10.1523/JNEUROSCI.05-08-02254.1985

[5] Halassa MM, Acsády L. Thalamic Inhibition: Diverse Sources, Diverse Scales. Trends in Neurosciences. 2016; 39: 680–693. https://doi.org/10.1016/j.tins.2016.08.001

[6] Fan D, Liao F, Wang Q. The pacemaker role of thalamic reticular nucleus in controlling spike-wave discharges and spindles. Chaos. 2017; 27: 073103. https://doi.org/10.1063/1.4991869

[7] Halassa MM, Chen Z, Wimmer RD, Brunetti PM, Zhao S, Zikopoulos B, et al. State-dependent architecture of thalamic reticular subnetworks. Cell. 2014; 158: 808–821. https://doi.org/10.1016/j.cell.2014.06.025

[8] Li Y, Lopez-Huerta VG, Adiconis X, Levandowski K, Choi S, Simmons SK, et al. Distinct subnetworks of the thalamic reticular nucleus. Nature. 2020; 583: 819–824. https://doi.org/10.1038/s41586-020-2504-5

[9] Bu J, Xu G, Zhou Y. Parvalbumin and Somatostatin Neurons in the Thalamic Reticular Nucleus Modulate Visual Information Processing in V1 of Mouse. Neuroscience Bulletin. 2025; 41: 1824–1842. https://doi.org/10.1007/s12264-025-01458-5

[10] Abdelaal MS, Midorikawa M, Suzuki T, Kobayashi K, Takata N, Miyata M, et al. Dysfunction of parvalbumin-expressing cells in the thalamic reticular nucleus induces cortical spike-and-wave discharges and an unconscious state. Brain Communications. 2022; 4: fcac010. https://doi.org/10.1093/braincomms/fcac010

[11] Wang XY, Xu X, Chen R, Jia WB, Xu PF, Liu XQ, et al. The thalamic reticular nucleus-lateral habenula circuit regulates depressive-like behaviors in chronic stress and chronic pain. Cell Reports. 2023; 42: 113170. https://doi.org/10.1016/j.celrep.2023.113170

[12] Steullet P, Cabungcal JH, Bukhari SA, Ardelt MI, Pantazopoulos H, Hamati F, et al. The thalamic reticular nucleus in schizophrenia and bipolar disorder: role of parvalbumin-expressing neuron networks and oxidative stress. Molecular Psychiatry. 2018; 23: 2057–2065. https://doi.org/10.1038/mp.2017.230

[13] Lee SH, Cox CL. Vasoactive intestinal peptide selectively depolarizes thalamic relay neurons and attenuates intrathalamic rhythmic activity. Journal of Neurophysiology. 2003; 90: 1224–1234. https://doi.org/10.1152/jn.00280.2003

[14] Burgunder JM, Heyberger B, Lauterburg T. Thalamic reticular nucleus parcellation delineated by VIP and TRH gene expression in the rat. Journal of Chemical Neuroanatomy. 1999; 17: 147–152. https://doi.org/10.1016/s0891-0618(99)00033-2

[15] McAlonan K, Cavanaugh J, Wurtz RH. Attentional modulation of thalamic reticular neurons. The Journal of Neuroscience: the Official Journal of the Society for Neuroscience. 2006; 26: 4444–4450. https://doi.org/10.1523/JNEUROSCI.5602-05.2006

[16] Wimmer RD, Schmitt LI, Davidson TJ, Nakajima M, Deisseroth K, Halassa MM. Thalamic control of sensory selection in divided attention. Nature. 2015; 526: 705–709. https://doi.org/10.1038/nature15398

[17] Halassa MM, Siegle JH, Ritt JT, Ting JT, Feng G, Moore CI. Selective optical drive of thalamic reticular nucleus generates thalamic bursts and cortical spindles. Nature Neuroscience. 2011; 14: 1118–1120. https://doi.org/10.1038/nn.2880

[18] Thankachan S, Katsuki F, McKenna JT, Yang C, Shukla C, Deisseroth K, et al. Thalamic Reticular Nucleus Parvalbumin Neurons Regulate Sleep Spindles and Electrophysiological Aspects of Schizophrenia in Mice. Scientific Reports. 2019; 9: 3607. https://doi.org/10.1038/s41598-019-40398-9

[19] Ni KM, Hou XJ, Yang CH, Dong P, Li Y, Zhang Y, et al. Selectively driving cholinergic fibers optically in the thalamic reticular nucleus promotes sleep. elife. 2016; 5: e10382. https://doi.org/10.7554/eLife.10382

[20] Jagirdar R, Fu CH, Park J, Corbett BF, Seibt FM, Beierlein M, et al. Restoring activity in the thalamic reticular nucleus improves sleep architecture and reduces Aβ accumulation in mice. Science Translational Medicine. 2021; 13: eabh4284. https://doi.org/10.1126/scitranslmed.abh4284

[21] Cumpana L, Zanoletti O, Kankanamge D, Copits B, Sandi C, Astori S. Corticotropin-releasing hormone modulates NREM sleep consolidation through the thalamic reticular nucleus. Nature Communications. 2025; 16: 7720. https://doi.org/10.1038/s41467-025-63118-6

[22] Raos VC, Savaki HE. Functional anatomy of the thalamic reticular nucleus as revealed with the [14C]deoxyglucose method following electrical stimulation and electrolytic lesion. Neuroscience. 1995; 68: 287–297. https://doi.org/10.1016/0306-4522(95)00113-w

[23] Perissinotti PP, Rivero-Echeto MC, Garcia-Rill E, Bisagno V, Urbano FJ. Leptin alters somatosensory thalamic networks by decreasing gaba release from reticular thalamic nucleus and action potential frequency at ventrobasal neurons. Brain Structure & Function. 2018; 223: 2499–2514. https://doi.org/10.1007/s00429-018-1645-x

[24] Scrocchi LA, Brown TJ, MaClusky N, Brubaker PL, Auerbach AB, Joyner AL, et al. Glucose intolerance but normal satiety in mice with a null mutation in the glucagon-like peptide 1 receptor gene. Nature Medicine. 1996; 2: 1254–1258. https://doi.org/10.1038/nm1196-1254

[25] Turton MD, O'Shea D, Gunn I, Beak SA, Edwards CM, Meeran K, et al. A role for glucagon-like peptide-1 in the central regulation of feeding. Nature. 1996; 379: 69–72. https://doi.org/10.1038/379069a0

[26] Secher A, Jelsing J, Baquero AF, Hecksher-Sørensen J, Cowley MA, Dalbøge LS, et al. The arcuate nucleus mediates GLP-1 receptor agonist liraglutide-dependent weight loss. The Journal of Clinical Investigation. 2014; 124: 4473–4488. https://doi.org/10.1172/JCI75276

[27] Kanoski SE, Fortin SM, Arnold M, Grill HJ, Hayes MR. Peripheral and central GLP-1 receptor populations mediate the anorectic effects of peripherally administered GLP-1 receptor agonists, liraglutide and exendin-4. Endocrinology. 2011; 152: 3103–3112. https://doi.org/10.1210/en.2011-0174

[28] Gong N, Xiao Q, Zhu B, Zhang CY, Wang YC, Fan H, et al. Activation of spinal glucagon-like peptide-1 receptors specifically suppresses pain hypersensitivity. The Journal of Neuroscience: the Official Journal of the Society for Neuroscience. 2014; 34: 5322–5334. https://doi.org/10.1523/JNEUROSCI.4703-13.2014

[29] Montaner M, Denom J, Jiang W, Magnan C, Trapp S, Gurden H. The local GLP-1 system in the olfactory bulb is required for odor-evoked cephalic phase of insulin release in mice. Molecular Metabolism. 2023; 73: 101738. https://doi.org/10.1016/j.molmet.2023.101738

[30] Shin YK, Martin B, Golden E, Dotson CD, Maudsley S, Kim W, et al. Modulation of taste sensitivity by GLP-1 signaling. Journal of Neurochemistry. 2008; 106: 455–463. https://doi.org/10.1111/j.1471-4159.2008.05397.x

[31] Williams EK, Chang RB, Strochlic DE, Umans BD, Lowell BB, Liberles SD. Sensory Neurons that Detect Stretch and Nutrients in the Digestive System. Cell. 2016; 166: 209–221. https://doi.org/10.1016/j.cell.2016.05.011

[32] Takai S, Yasumatsu K, Inoue M, Iwata S, Yoshida R, Shigemura N, et al. Glucagon-like peptide-1 is specifically involved in sweet taste transmission. FASEB Journal: Official Publication of the Federation of American Societies for Experimental Biology. 2015; 29: 2268–2280. https://doi.org/10.1096/fj.14-265355

[33] McClean PL, Hölscher C. Liraglutide can reverse memory impairment, synaptic loss and reduce plaque load in aged APP/PS1 mice, a model of Alzheimer's disease. Neuropharmacology. 2014; 76: 57–67. https://doi.org/10.1016/j.neuropharm.2013.08.005

[34] McClean PL, Parthsarathy V, Faivre E, Hölscher C. The diabetes drug liraglutide prevents degenerative processes in a mouse model of Alzheimer's disease. The Journal of Neuroscience: the Official Journal of the Society for Neuroscience. 2011; 31: 6587–6594. https://doi.org/10.1523/JNEUROSCI.0529-11.2011

[35] During MJ, Cao L, Zuzga DS, Francis JS, Fitzsimons HL, Jiao X, et al. Glucagon-like peptide-1 receptor is involved in learning and neuroprotection. Nature Medicine. 2003; 9: 1173–1179. https://doi.org/10.1038/nm919

[36] Cork SC, Richards JE, Holt MK, Gribble FM, Reimann F, Trapp S. Distribution and characterisation of Glucagon-like peptide-1 receptor expressing cells in the mouse brain. Molecular Metabolism. 2015; 4: 718–731. https://doi.org/10.1016/j.molmet.2015.07.008

[37] Lein ES, Hawrylycz MJ, Ao N, Ayres M, Bensinger A, Bernard A, et al. Genome-wide atlas of gene expression in the adult mouse brain. Nature. 2007; 445: 168–176. https://doi.org/10.1038/nature05453

[38] Zikopoulos B, Barbas H. Prefrontal projections to the thalamic reticular nucleus form a unique circuit for attentional mechanisms. The Journal of Neuroscience: the Official Journal of the Society for Neuroscience. 2006; 26: 7348–7361. https://doi.org/10.1523/JNEUROSCI.5511-05.2006

[39] Kakei S, Na J, Shinoda Y. Thalamic terminal morphology and distribution of single corticothalamic axons originating from layers 5 and 6 of the cat motor cortex. The Journal of Comparative Neurology. 2001; 437: 170–185. https://doi.org/10.1002/cne.1277

[40] Graham DL, Durai HH, Trammell TS, Noble BL, Mortlock DP, Galli A, et al. A novel mouse model of glucagon-like peptide-1 receptor expression: A look at the brain. The Journal of Comparative Neurology. 2020; 528: 2445–2470. https://doi.org/10.1002/cne.24905

[41] Crabtree JW. Functional Diversity of Thalamic Reticular Subnetworks. Frontiers in Systems Neuroscience. 2018; 12: 41. https://doi.org/10.3389/fnsys.2018.00041

[42] Williamson RS, Polley DB. Parallel pathways for sound processing and functional connectivity among layer 5 and 6 auditory corticofugal neurons. elife. 2019; 8: e42974. https://doi.org/10.7554/eLife.42974

[43] Bourassa J, Pinault D, Deschênes M. Corticothalamic projections from the cortical barrel field to the somatosensory thalamus in rats: a single-fibre study using biocytin as an anterograde tracer. The European Journal of Neuroscience. 1995; 7: 19–30. https://doi.org/10.1111/j.1460-9568.1995.tb01016.x

[44] Bourassa J, Deschênes M. Corticothalamic projections from the primary visual cortex in rats: a single fiber study using biocytin as an anterograde tracer. Neuroscience. 1995; 66: 253–263. https://doi.org/10.1016/0306-4522(95)00009-8

[45] Liu Y, Bech P, Tamura K, Délez LT, Crochet S, Petersen CCH. Cell class-specific long-range axonal projections of neurons in mouse whisker-related somatosensory cortices. elife. 2024; 13: RP97602. https://doi.org/10.7554/eLife.97602

[46] Einav A, Azouz R. Corticothalamic modulation of somatosensory thalamic tactile processing. The Journal of Physiology. 2025; 603: 2801–2819. https://doi.org/10.1113/JP287526

[47] Mo C, Sherman SM. A Sensorimotor Pathway via Higher-Order Thalamus. The Journal of Neuroscience: the Official Journal of the Society for Neuroscience. 2019; 39: 692–704. https://doi.org/10.1523/JNEUROSCI.1467-18.2018

[48] Wang W, Andolina IM, Lu Y, Jones HE, Sillito AM. Focal Gain Control of Thalamic Visual Receptive Fields by Layer 6 Corticothalamic Feedback. Cerebral Cortex. 2018; 28: 267–280. https://doi.org/10.1093/cercor/bhw376

[49] Crandall SR, Cruikshank SJ, Connors BW. A corticothalamic switch: controlling the thalamus with dynamic synapses. Neuron. 2015; 86: 768–782. https://doi.org/10.1016/j.neuron.2015.03.040

[50] Kim A, Latchoumane C, Lee S, Kim GB, Cheong E, Augustine GJ, et al. Optogenetically induced sleep spindle rhythms alter sleep architectures in mice. Proceedings of the National Academy of Sciences of the United States of America. 2012; 109: 20673–20678. https://doi.org/10.1073/pnas.1217897109

[51] Steriade M, Timofeev I. Neuronal plasticity in thalamocortical networks during sleep and waking oscillations. Neuron. 2003; 37: 563–576. https://doi.org/10.1016/s0896-6273(03)00065-5

[52] Hua MH, Chen YL, Chen MH, Huang KL, Hsu JW, Bai YM, et al. Network-Specific Corticothalamic Dysconnection in Attention-Deficit Hyperactivity Disorder. Journal of Developmental and Behavioral Pediatrics. 2021; 42: 122–127. https://doi.org/10.1097/DBP.0000000000000875

[53] Trenado C, Haab L, Strauss DJ. Corticothalamic feedback dynamics for neural correlates of auditory selective attention. IEEE Transactions on Neural Systems and Rehabilitation Engineering: a Publication of the IEEE Engineering in Medicine and Biology Society. 2009; 17: 46–52. https://doi.org/10.1109/TNSRE.2008.2010469

[54] Sunahara M, Rios A, Kawabata M, Kato S, Hamada S, Ohtsuka T, et al. Temporally Coordinated Activity among Motor Cortex, Thalamus, and Thalamic Reticular Nucleus Neurons during Rat Forelimb Movements. The Journal of Neuroscience: the Official Journal of the Society for Neuroscience. 2026; 46: e1827252026. https://doi.org/10.1523/JNEUROSCI.1827-25.2026

[55] Jennings JH, Rizzi G, Stamatakis AM, Ung RL, Stuber GD. The inhibitory circuit architecture of the lateral hypothalamus orchestrates feeding. Science (New York, N.Y.). 2013; 341: 1517–1521. https://doi.org/10.1126/science.1241812

[56] Burdakov D, Karnani MM, Gonzalez A. Lateral hypothalamus as a sensor-regulator in respiratory and metabolic control. Physiology & Behavior. 2013; 121: 117–124. https://doi.org/10.1016/j.physbeh.2013.03.023

[57] Burt J, Alberto CO, Parsons MP, Hirasawa M. Local network regulation of orexin neurons in the lateral hypothalamus. American Journal of Physiology. Regulatory, Integrative and Comparative Physiology. 2011; 301: R572–R580. https://doi.org/10.1152/ajpregu.00674.2010

[58] Saper CB, Chou TC, Scammell TE. The sleep switch: hypothalamic control of sleep and wakefulness. Trends in Neurosciences. 2001; 24: 726–731. https://doi.org/10.1016/s0166-2236(00)02002-6

[59] Liu K, Kim J, Kim DW, Zhang YS, Bao H, Denaxa M, et al. Lhx6-positive GABA-releasing neurons of the zona incerta promote sleep. Nature. 2017; 548: 582–587. https://doi.org/10.1038/nature23663

[60] Zhang X, van den Pol AN. Rapid binge-like eating and body weight gain driven by zona incerta GABA neuron activation. Science (New York, N.Y.). 2017; 356: 853–859. https://doi.org/10.1126/science.aam7100

[61] Falasconi A, Arber S. Basal ganglia-brainstem interactions. Current Biology. 2025; 35: R1004–R1010. https://doi.org/10.1016/j.cub.2025.07.019

[62] Chen ZK, Dong H, Liu CW, Liu WY, Zhao YN, Xu W, et al. A cluster of mesopontine GABAergic neurons suppresses REM sleep and curbs cataplexy. Cell Discovery. 2022; 8: 115. https://doi.org/10.1038/s41421-022-00456-5

[63] Foster NN, Barry J, Korobkova L, Garcia L, Gao L, Becerra M, et al. The mouse cortico-basal ganglia-thalamic network. Nature. 2021; 598: 188–194. https://doi.org/10.1038/s41586-021-03993-3

[64] Velayos JL, Reinoso-Suárez F. Prosencephalic afferents to the mediodorsal thalamic nucleus. The Journal of Comparative Neurology. 1985; 242: 161–181. https://doi.org/10.1002/cne.902420203

[65] de Bourbon-Teles J, Bentley P, Koshino S, Shah K, Dutta A, Malhotra P, et al. Thalamic control of human attention driven by memory and learning. Current Biology. 2014; 24: 993–999. https://doi.org/10.1016/j.cub.2014.03.024

[66] Groos D, Helmchen F. The lateral habenula: A hub for value-guided behavior. Cell Reports. 2024; 43: 113968. https://doi.org/10.1016/j.celrep.2024.113968

[67] Michel L, Molina P, Mameli M. The behavioral relevance of a modular organization in the lateral habenula. Neuron. 2024; 112: 2669–2685. https://doi.org/10.1016/j.neuron.2024.04.026

[68] Merchant W, Tinajero A, Khan A, Chu Y, Saleh S, Tasabehji D, et al. RYGB induces vagal sensory neuropathy characterized by altered Glp1r expression and enhanced exendin-4 responsiveness in male mice. American Journal of Physiology. Endocrinology and Metabolism. 2026; 330: E114–E126. https://doi.org/10.1152/ajpendo.00452.2025